



Effect of flue gas cooler and overlap energy utilization on supercritical carbon dioxide coal fired power plant

Zhaofu Wang^a, Enhui Sun^{a,b}, Jinliang Xu^{a,b,*}, Chao Liu^a, Guanglin Liu^a

^a Beijing Key Laboratory of Multiphase Flow and Heat Transfer for Low Grade Energy Utilization, North China Electric Power University, Beijing 102206, China

^b Key Laboratory of Condition Monitoring and Control for Power Plant Equipment of Ministry of Education, North China Electric Power University, Beijing 102206, China

ARTICLE INFO

Keywords:

sCO₂ cycle
Flue gas cooler
Overlap energy utilization
Cascade energy utilization
Thermodynamics cycle

ABSTRACT

Supercritical carbon dioxide (sCO₂) cycle is suitable for high temperature heat source, but introduces challenging in absorbing moderate/low temperature flue gas energy for coal fired power plant. Here, we explore the effect of flue gas cooler (FGC) and overlap energy utilization (OEU) on sCO₂ cycle. FGC and OEU extract moderate temperature flue gas energy by a splitting CO₂ flow rate from the cycle and a combined cycle, respectively. Recompression cycle plus reheating (RC + RH) and tri-compression cycle plus reheating (TC + RH) are two basic cycle types for coal fired power plant. A thermodynamics model coupling with thermal-hydraulic characteristic is developed. The analysis is performed for a 100 MW rated power capacity. For RC + RH, we show that OEU yields an electric power efficiency increment of 0.13% compared to FGC, which is caused by smaller pressure drops in boiler components when using OEU. Even though TC + RH introduces difficulty in absorbing moderate/low temperature flue gas energy, OEU still can decrease outlet flue gas temperature ($T_{fg,ex}$) to 126 °C, which is acceptable. However, FGC achieves a higher $T_{fg,ex}$ of 172.6 °C by a pinch temperature difference limit of 30 °C, which deteriorates boiler efficiency thus it is not acceptable. We conclude that OEU is better than FGC, no matter for RC + RH or TC + RH. The double-channel-tail-flue concept is proposed to not only increase thermal efficiency of the system, but also elevate boiler efficiency. This paper presents an important clue to design thermodynamics cycle for small capacity coal fired power plant, which is expected to have fast response with respect to load variations.

1. Introduction

Supercritical carbon dioxide cycle (sCO₂) was proposed by Sulzer in 1950 [1]. The sCO₂ cycle was not paid much attention since its initial proposal, but great progresses have been made on sCO₂ cycle recently [2]. The heat source to drive a sCO₂ cycle can be nuclear energy [3-7], solar energy [8-12], waste heat [13-16], and fossil energy (nature gas and coal) [17-21]. The research and development (R&D) on fossil energy driven sCO₂ cycle comes from the demand in developing power plants with fast response to load variations. Due to the increased utilization of renewable energy [22], the electric grid will be operating in a mixing mode to include various energy sources of renewable, nuclear and fossil. Commercial power plants operating in water-steam Rankine cycle slowly respond to load variations. The different change speeds of load variations between fossil energy and renewable energy account for

the “wind and solar curtailment” phenomenon [23]. Compared with water-steam Rankine cycle, sCO₂ cycle not only has higher efficiency, but also has quick response to load variations due to simplified system design [24].

There does not exist a fixed sCO₂ cycle that can be suitable for all the heat sources [24]. For instance, due to narrow temperature range of heat source coupling with the cycle, recompression cycle (RC) is suitable for nuclear energy and solar energy, but is not suitable for waste heat [25]. Xu et al. [26] commented on key issues when sCO₂ cycle is applied for coal fired power plant. First, mass flow rate is significantly larger for sCO₂ cycle compared to water-steam Rankine cycle, noting that mass flow rate is scaled as $m \sim \Delta h^{-1}$ where Δh is the enthalpy difference of working fluid across a boiler. For sCO₂ cycle, the much smaller Δh yields ultra-large mass flow rate and significantly larger pressure drop in various heat exchangers. To overcome this difficulty, Xu et al. [26] proposed the module boiler design, by which pressure drops for sCO₂

* Corresponding author at: Beijing Key Laboratory of Multiphase Flow and Heat Transfer for Low Grade Energy Utilization, North China Electric Power University, Beijing 102206, China.

E-mail address: xjl@ncepu.edu.cn (J. Xu).

<https://doi.org/10.1016/j.enconman.2021.114866>

Received 3 August 2021; Received in revised form 6 October 2021; Accepted 9 October 2021

Available online 23 October 2021

0196-8904/© 2021 Elsevier Ltd. All rights reserved.

Nomenclature			
B	coal consumption rate, kg/s	exg	exhaust flue gas
d	diameter, m	f	fluid; friction
e	exergy, kJ/kg	fg	flue gas
f	friction coefficient	fh	fly ash after coal fired
G	mass flux, kg/m ² s	flame	theoretical combustion
h	enthalpy per unit mass, kJ/kg	H	high temperature
H	height, m	h	high temperature side
I	exergy destruction, MW	i	inner of tube; inlet of medium temperature flue gas heater; the i -th species
l	length of component, m	L	low temperature
m	mass flow rate, kg/s	M	medium temperature
P	pressure, MPa	net	net power output
Pr	Prandtl number	o	outer of tube; outlet of medium temperature flue gas heater
q	heat absorption per unit mass flow rate, kW/kg;	pri	primary
Q	thermal load, MW; heating value, kJ/kg	sec	secondary
Re	Reynolds number	th	thermal
s	entropy per unit mass, kJ/kg;	<i>Abbreviation</i>	
T	temperature, °C	AP	air preheater
w	output/input work per unit mass, kJ/kg;	C1	the main compressor
W	output/input work, MW	C2	the auxiliary compressor
x	split ratio	EAP	external air preheater
<i>Greek symbols</i>		FGC	flue gas cooler; a method to absorb residual flue gas heat which a flue gas cooler is arranged in boiler tail flue
α	boiler heat retention coefficient	LCW	lower part of cooling wall
Δ	difference; absolute roughness of tubes, mm	LHV	lower heating value
ΔP	pressure drop, MPa	LTR	low-temperature recuperator
η	efficiency	OEU	overlap energy utilization
ρ	density, kg/m ³	RC	recompression cycle
λ	thermal conductivity, W/(mK)	RH	reheating
ϕ	the ratio of the volume of i -th species to the total flue gas volume	RH1	reheater 1
<i>Subscripts</i>		sC	simple cycle
0	environment	SH1	superheater 1
1, 2, 3...	state points	T1	the high pressure turbine
ar	received basis of the designed coal	T2	the low pressure turbine
cal	calculated value	TC	tri-compression cycle
e	electric power	UCW	upper part of cooling wall

cycle can be decreased to a similar level as those of water-steam Rankine cycle.

The second issue is the extraction of flue gas energy over entire temperature range [26]. Combusting coal generates ~1500 °C flue gas, while the outlet flue gas temperature discharged to environment should be as low as possible (for example, ~120 °C). Hence, a sCO₂ cycle should absorb flue gas energy within a wide temperature range of (1500–120) °C. Extraction of flue gas energy over entire temperature range shall satisfy the cascade energy utilization principle. In the literature, there are two methods to achieve this target. A flue gas cooler (FGC) extracts a portion of CO₂ flow rate somewhere in a sCO₂ cycle (for example, from a compressor outlet), heats the splitting CO₂ stream by moderate temperature flue gas, and then mixes with the main CO₂ stream somewhere of the cycle [27–30]. Therefore, flue gas energy in high, moderate and low temperature range is absorbed by the main sCO₂ cycle, a FGC and an air-preheater (AP), respectively, satisfying the cascade energy utilization principle. Xu et al. [26] commented on the effect of different extraction point and re-mixing point on cycle performance. FGC can decrease the outlet flue gas temperature to a significantly low level, raising the boiler efficiency, but slightly decrease the system thermal efficiency due to more heat added to the cycle.

Alternatively, a combined sCO₂ cycle absorbs flue gas energy over entire temperature range. A top cycle and a bottom cycle absorb high

and moderate temperature flue gas energy, respectively [31]. The overlap energy utilization is proposed to fill the efficiency gap between the two cycles [32]. The top cycle absorbs high temperature flue gas heat, but the bottom cycle not only absorbs moderate temperature flue gas heat, but also absorbs a portion of high temperature flue gas heat. Hence, the bottom cycle efficiency is raised to improve the global efficiency of the system. The utilization of two cycles introduces more components in the system. To simplify the system design, the components sharing technique was proposed [32]. The analysis for a 1000 MW power plant shows the improved system efficiency by using overlap energy utilization compared to cascade energy utilization.

The above descriptions comment on the absorption of flue gas energy over entire temperature range. Now, we comment on the cycle that can be used for coal fired power plant. RC is widely applied for various heat sources [9,33,34]. One may ask a question that is RC the best cycle for thermal-power conversion? To answer this question, Sun et al. [35] introduces synergetics to construct multi-compressions sCO₂ cycle. The analysis starts from the decoupling of a RC into two simplified simple Brayton cycles (sCs, each sC contains one heater, one compressor, one turbine, one recuperator and one cooler). It is seen that RC has higher efficiency than a single sC. The cooperative interaction of the two sCs can be regarded as the extra heat of the whole system is only dissipated to environment by the first sC, while the extra heat of the second sC is

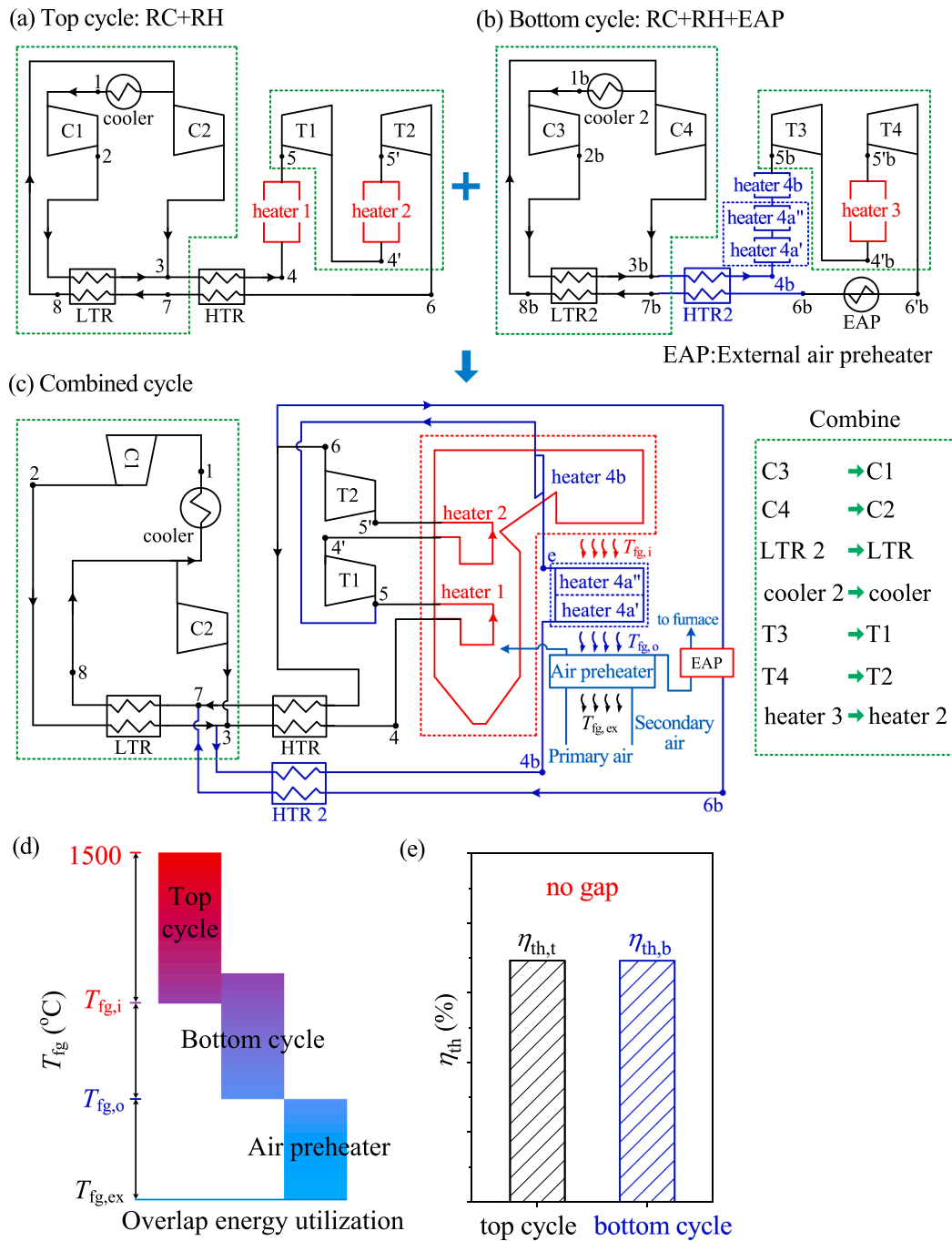


Fig. 1. RC + RH with overlap energy utilization (OEU) (a: top cycle; b: bottom cycle; c: combined cycle after components sharing; d: overlap energy utilization; e: equal efficiency for top cycle and bottom cycle for OEU. This figure is cited from Ref. [37]. Copyright 2020, Elsevier.)

dissipated to the first sC, not to environment. Hence, the mean efficiency of the second sC can be 1. Multi-compressions sCO₂ cycle can be constructed in a similar way. For instance, the tri-compressions cycle (TC) is built by cooperation between a RC and a sC. At the main vapor parameters 550 °C/20 MPa, thermal efficiencies are increased from 47.43% for RC to 49.47% for TC. Other techniques such as intercooling and reheating also improve the system performance. It is shown that intercooling only has weak influence on efficiency, thus it is not considered in this paper [26]. However, reheating apparently elevates the absorption temperature of a cycle [26], hence it is adopted in this paper.

The above comments indicate that FGC reflects cascade energy utilization, improving boiler efficiency but weakens thermal efficiency of

the system. Overlap energy utilization (OEU) uses a combined cycle to extract flue gas energy. Compared to conventional combined cycle, OEU sufficiently utilizes the high quality of flue gas energy in high temperature zone, even for bottom cycle. Hence, OEU is useful to maximize the whole system efficiency.

The objective of this paper is to perform a comprehensive study regarding the effect of FGC and OEU on cycle performance. Different from our previous papers focusing on 1000 MW power capacity [26,31,32], we present the analysis for 100 MW coal fired power plant in this paper. This is because small capacity such as 100 MW is believed to have faster response to load variations, which is helpful to balance dynamic features between fossil energy and renewable energies [36]. The present paper contains three major parts. The first part deals with the

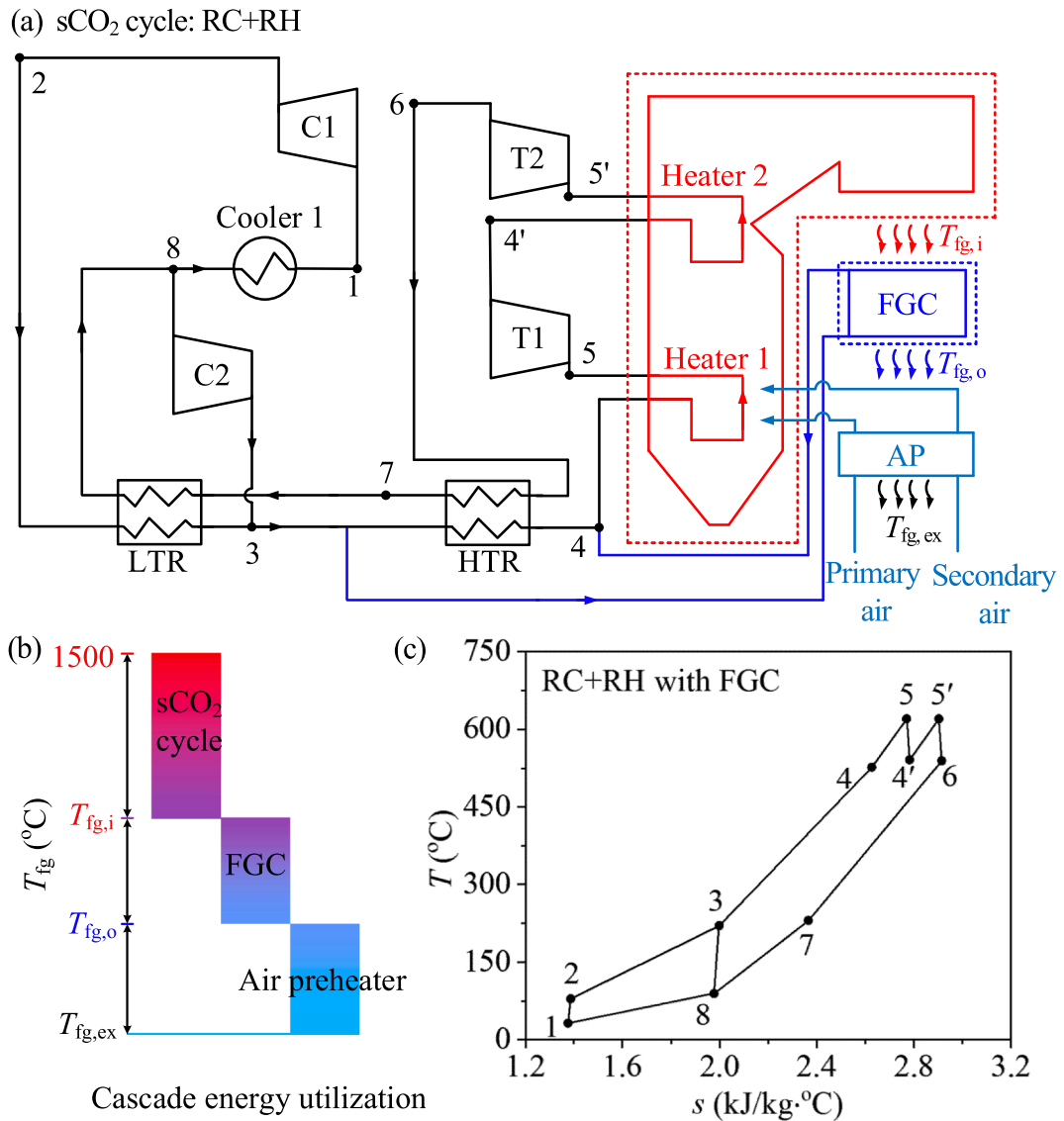


Fig. 2. RC + RH with flue gas cooler (FGC) (a: RC + RH with FGC; b: cascade energy utilization; c: T-s curves).

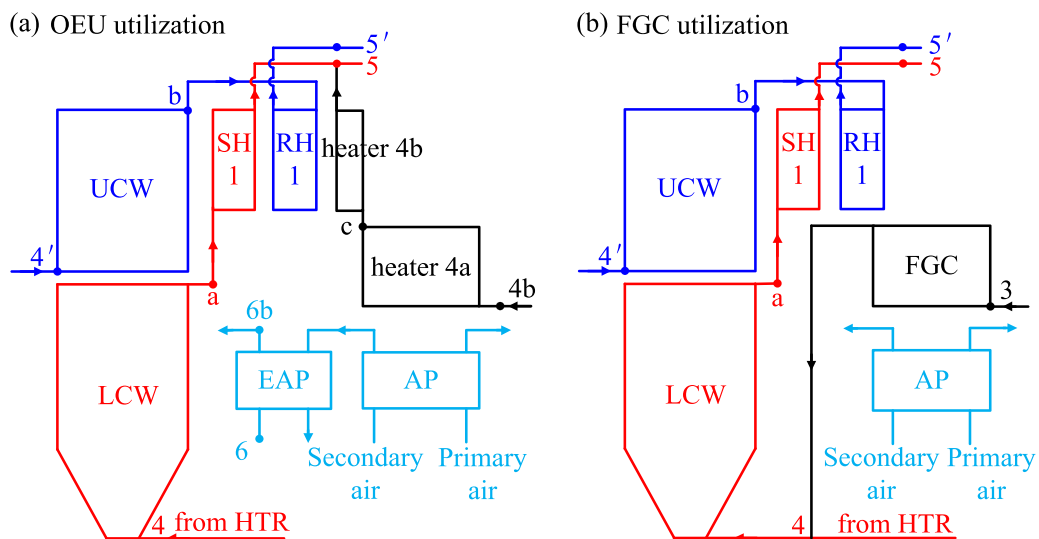


Fig. 3. Arrangement of boiler components for RC + RH with OEU (a) and FGC (b).

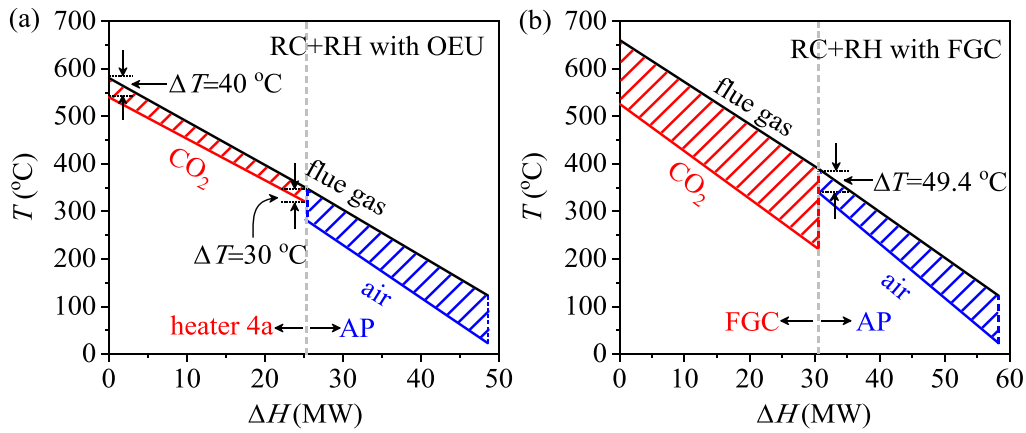


Fig. 4. T - ΔH curves for heat exchangers (heater 4a or FGC) operating in moderate temperature flue gas region and AP operating in low temperature flue gas region.

comparison of FGC and OEU using RC + RH (recompression $s\text{CO}_2$ cycle plus reheating) corresponding to Figs. 1-7. The second part regards the comparison of FGC and OEU using TC + RH (tri-compressions $s\text{CO}_2$ cycle plus reheating), corresponding to Figs. 8-13. We conclude that OEU is better than FGC, no matter for RC or TC. In order to reach the target of both high thermal efficiency of TC and low outlet flue gas temperature (corresponding to high boiler efficiency), a new technique called the double-channel-tail-flue is proposed in the end of this paper (see Fig. 14).

The originality of the present paper is stated as follows. First, our previous studies focus on the concept design and analysis of 1000 MW S-CO_2 coal fired power plant [26,31,32]. OEU and FGC were separately investigated regarding their effects on the thermal performance of the 1000 MW power plant [27,28,32]. The present paper deals with 100 MW S-CO_2 coal fired power plant. When the power capacity is decreased by one magnitude, the boiler design is significantly changed. For example, for 1000 MW power plant, modular boiler design should be used to decrease ultra-large pressure drop induced by ultra-large flow rate [26]. However, it is not necessary to adopt the modular boiler design for small capacity such as 100 MW [37]. Hence, the present paper tries to answer the question that what are the effects of OEU and FGC on power plant performance with small capacity such as 100 MW. Second, our previous studies analyzed the effect of OEU and FGC on the S-CO_2 power plant when the basic cycle type is chosen as RC + RH [33,37] or RC + DRH [21,27,32]. TC is proposed in ref. [35] to improve the cycle efficiency for S-CO_2 cycle. However, it is not clear how and why OEU and FGC influence the design and operation of S-CO_2 coal fired power plant when TC cycle is adopted in the thermal system. The above two issues are solved and answered in the present paper.

2. System description

2.1. RC + RH for overlap energy utilization

RC + RH for overlap energy utilization is a combined cycle containing a top cycle (see Fig. 1a) and a bottom cycle (see Fig. 1b). Both of them use RC + RH. Overlap energy utilization (OEU) includes an overlap region setting in high temperature zone. Thus, major portion of flue gas energy in high temperature zone is extracted by the top cycle, small portion of flue gas energy in high temperature zone is absorbed by the bottom cycle. Flue gas energy in moderate temperature zone is absorbed by the bottom cycle. Flue gas energy in low temperature zone is extracted by air-preheater (AP), see Fig. 1d, where $T_{fg,i}$ and $T_{fg,o}$ are two interface temperatures, $T_{fg,ex}$ is the outlet flue gas temperature. OEU ensures same pressure and temperature for some components of top and bottom cycle. For example, T_5 and T_4 across T1 in top cycle equal to T_{5b} and T_{4b} across T3 in bottom cycle. Hence, T3 in bottom cycle can be

combined into T1 in top cycle, which is called the components sharing to simplify the system design. Other components sharing is seen in Fig. 1c. It is noted that not all the components can be shared by the two cycles. For example, Heater 4a, 4a' and 4b independently exist in bottom cycle (see Fig. 1c). The overlap energy utilization (OEU) ensures no efficiency gap between top cycle and bottom cycle (see Fig. 1e) [37].

2.2. RC + RH with flue gas cooler

Fig. 2a shows RC + RH with flue gas cooler (FGC). Different from OEU, only one cycle of RC + RH is used without using a bottom cycle. The FGC method reflects cascade energy utilization with flue gas temperatures consecutively changing from high to low without setting an overlap region. The three regions of flue gas energies are extracted by the main RC + RH cycle, a FGC and an AP (see Fig. 2b). Fig. 2c shows the T - s diagram.

2.3. The $s\text{CO}_2$ boiler

Considering the cycles shown in Figs. 1-2 are coupling with $s\text{CO}_2$ boiler, the boiler should be decoupled into various heat exchangers. Let's deal with OEU first, heater 1 in Fig. 1 consists of two components of LCW (lower part of cooling wall) and SH1 (superheater 1). Heater 2 is decoupled into UCW (upper part of cooling wall) and RH1 (reheater 1), see Fig. 3a. Other components are also shown in Fig. 3a. For FGC utilization, heaters 1 and 2 are decoupled into four components that are similar to the OEU utilization (see Fig. 3b). We shall note the major difference of components arranged in tail flue for OEU and FGC. For the former, heater 4b extracts high temperature flue gas energy, heater 4a exists in tail flue, together with an external air-preheater (EAP). For the latter, FGC is in tail flue. Both methods need AP to extract low temperature flue gas energy.

3. Numerical model

The cycle is strongly coupled with thermal-hydraulic characteristic of boiler, consisting of three levels of iterations for flue gas temperature at furnace outlet (T_{fl}), pressure drops in boiler tubes, and thermal load conservation of the system (see Figs. A1-A3). Once initial parameters are given (see Table 1), pressure drops in various heaters of boiler are assumed. Then, the thermodynamic cycle subroutine is called. The first level of T_{fl} is performed to achieve boiler parameters such as volume heat flux q_v and heat flux over furnace cross-section q_a . The computation is continued by the second level of iteration of pressure drops. The calculation is stopped until the thermal load is conserved between cycle side and furnace side.

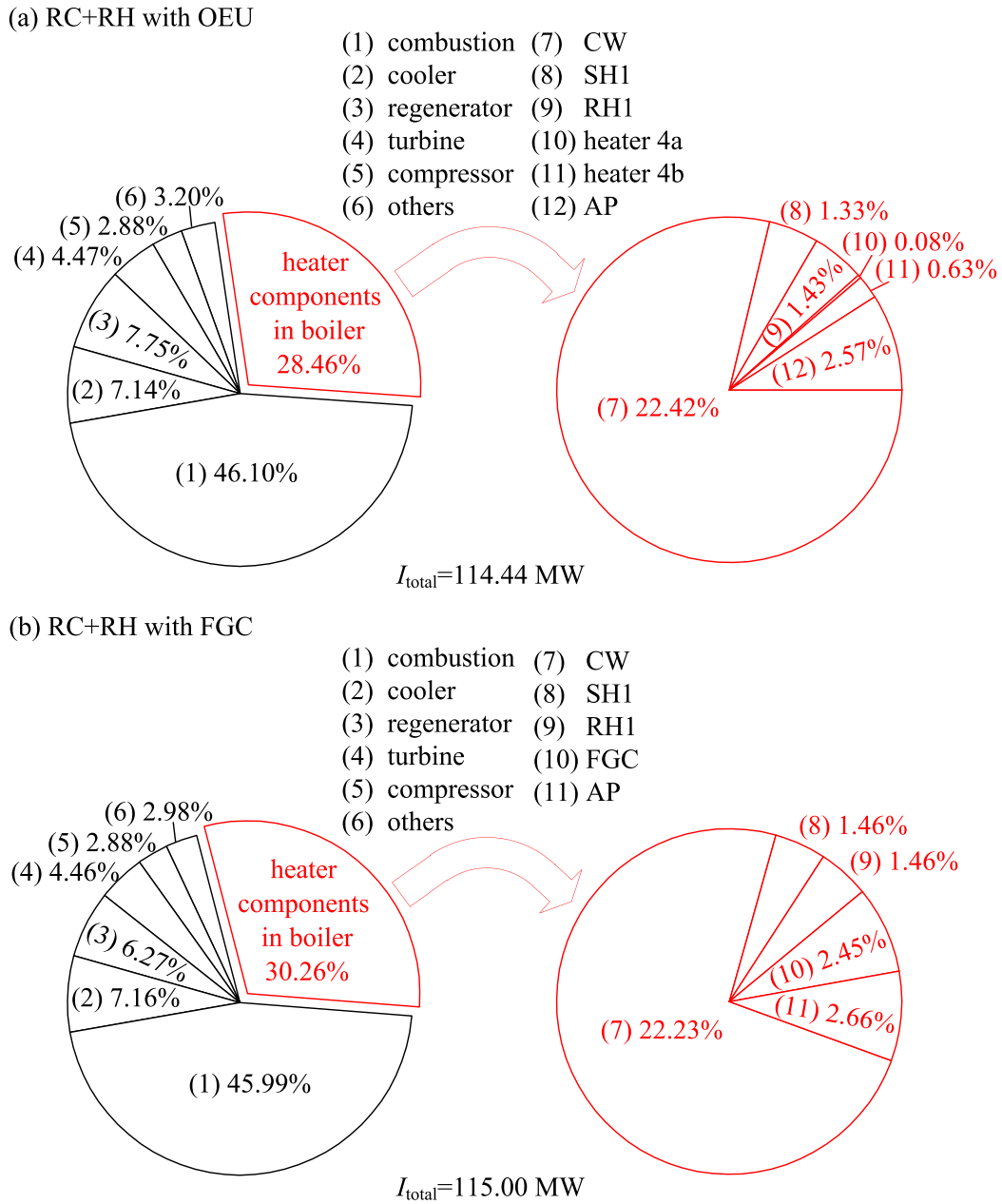


Fig. 5. Exergy destruction distributions for RC + RH with OEU (a) and FGC (b).

3.1. Computation of sCO₂ cycle

The cycle computation needs to deal with cascade or overlap energy utilization, involving two junction temperatures of flue gas, $T_{fg,i}$ and $T_{fg,o}$. Specified by the pinch temperature difference, $T_{fg,i}$ and $T_{fg,o}$ are related to the CO₂ temperatures in tube side with $T_{fg,i} \geq T_{CO_2} + 40$ and $T_{fg,o} \geq T_{CO_2} + 30$ at corresponding points. Thermal loads in high, moderate and low temperature regions are $Q_{fg,H}$, $Q_{fg,M}$ and $Q_{fg,L}$, respectively:

$$Q_{fg,H} = B_{cal} \cdot (h_{flame} - h_{fg,i}) \quad (1)$$

$$Q_{fg,M} = B_{cal} \cdot (h_{fg,i} - h_{fg,o}) \quad (2)$$

$$Q_{fg,L} = B_{cal} \cdot (h_{fg,o} - h_{exg}) \quad (3)$$

where B_{cal} is the coal consumption rate, h_{flame} is the flue gas enthalpy at the flame temperature, $h_{fg,i}$, $h_{fg,o}$ and h_{exg} are the flue gas enthalpies at

$T_{fg,i}$, $T_{fg,o}$ and $T_{fg,ex}$ respectively.

For RC + RH with OEU, thermal load of $Q_{heater\ 4a}$ in moderate temperature region is

$$\alpha \cdot Q_{fg,M} = Q_{heater\ 4a} \quad (4)$$

$$Q_{heater4a} = x_{heater4a} m_{CO_2} \cdot (h_c - h_{4b}) \quad (5)$$

where α is the boiler heat retention coefficient, $x_{heater\ 4a}$ is the ratio of flow rate in heater 4a to the total CO₂ flow rate of m_{CO_2} .

The computation for OEU is

$$w_{net} = (w_{T1} + w_{T2}) - (w_{C1} + w_{C2}) \quad (6)$$

$$q_{total} = (1 - x_{heater\ 4}) (h_5 - h_4) + x_{heater\ 4} (h_5 - h_{4b}) + (h_5' - h_4') - x_{EAP} (h_6 - h_{6b}) \quad (7)$$

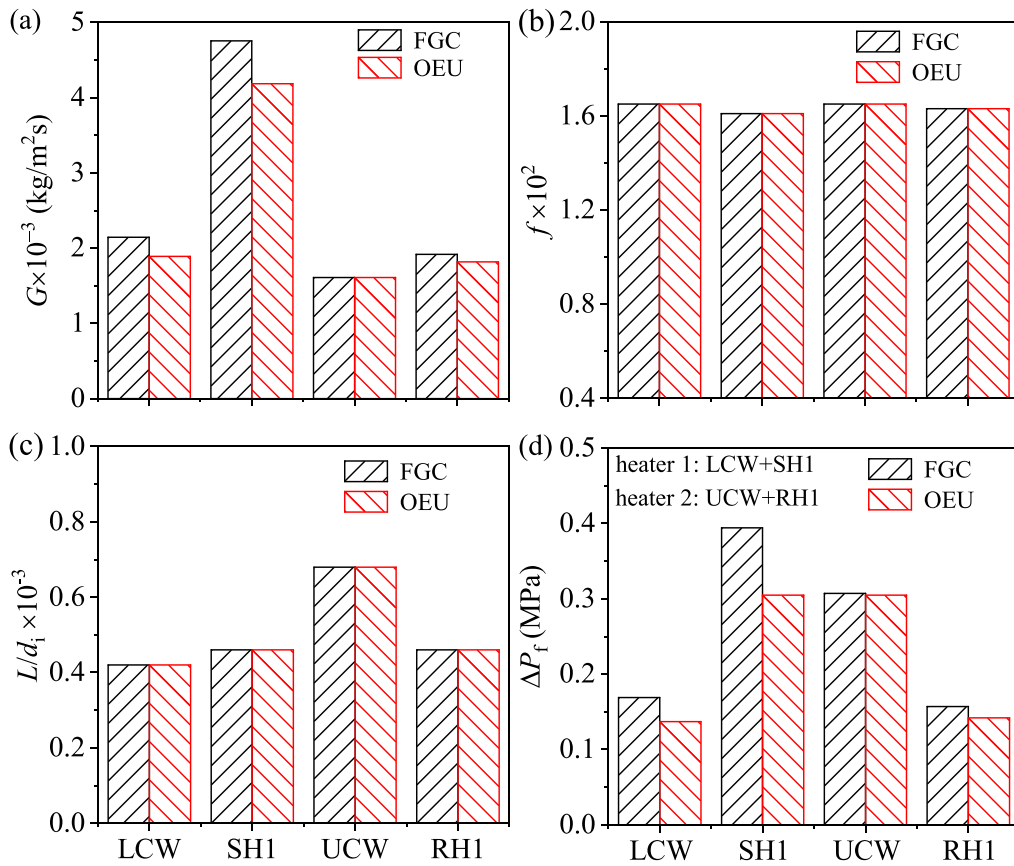


Fig. 6. Factors influencing pressure drops for RC + RH with OEU and FGC (a: mass fluxes in tubes; b: frictional coefficients; c: length to diameter ratio of tubes; d: frictional pressure drops in boiler components).

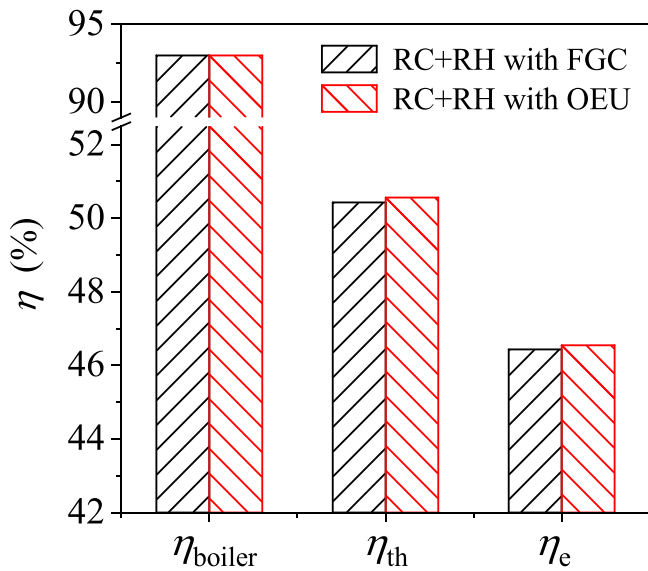


Fig. 7. Boiler efficiency, thermal efficiency and electric power efficiency for RC + RH with FGC and OEU.

$$\eta_{th} = \frac{W_{net}}{q_{total}}, m_{CO_2} = \frac{W_{net}}{w_{net}} \quad (8)$$

where w_{net} is net power per unit mass flow rate of CO_2 , q_{total} is total heat absorption per unit mass flow rate of CO_2 , x_{EAP} is the ratio of flow rate in EAP to the total flow rate, W_{net} is power capacity ($W_{net} = 100$ MW in the paper).

For RC + RH with FGC, thermal load Q_{FGC} is

$$\alpha \cdot Q_{fg,M} = Q_{FGC}, Q_{FGC} = x_{FGC} \cdot m_{CO_2} \cdot (h_4 - h_3) \quad (9)$$

where x_{FGC} is the ratio of flow rate in FGC to the total flow rate of CO_2 .

The computation for FGC is

$$w_{net} = (w_{T1} + w_{T2}) - (w_{C1} + w_{C2}) \quad (11)$$

$$q_{total} = (h_5 - h_4) + x_{FGC}(h_4 - h_3) + (h_{5'} - h_{4'}) \quad (12)$$

$$\eta_{th} = \frac{W_{net}}{q_{total}} \quad (13)$$

Specific exergy per unit mass flow rate is calculated as $e = h - T_0s$, where T_0 is the environment temperature, s is the entropy per unit mass flow rate. Exergy losses per unit mass flow rate in various components are shown in Table 2. The input exergy of system e_{in} equals to the chemical exergy of coal [37]:

$$e_{in} = Q_{LHV} \left(1.0064 + 0.1519 \frac{H_{ar}}{C_{ar}} + 0.0616 \frac{O_{ar}}{C_{ar}} + 0.0429 \frac{N_{ar}}{C_{ar}} \right) \quad (14)$$

where Q_{LHV} is the low heating value of design coal per unit mass. C_{ar} , H_{ar} , O_{ar} and N_{ar} are the ratios of C (carbon), H (hydrogen), O(oxygen) and N (nitrogen) on the received basis of designed coal, respectively (see

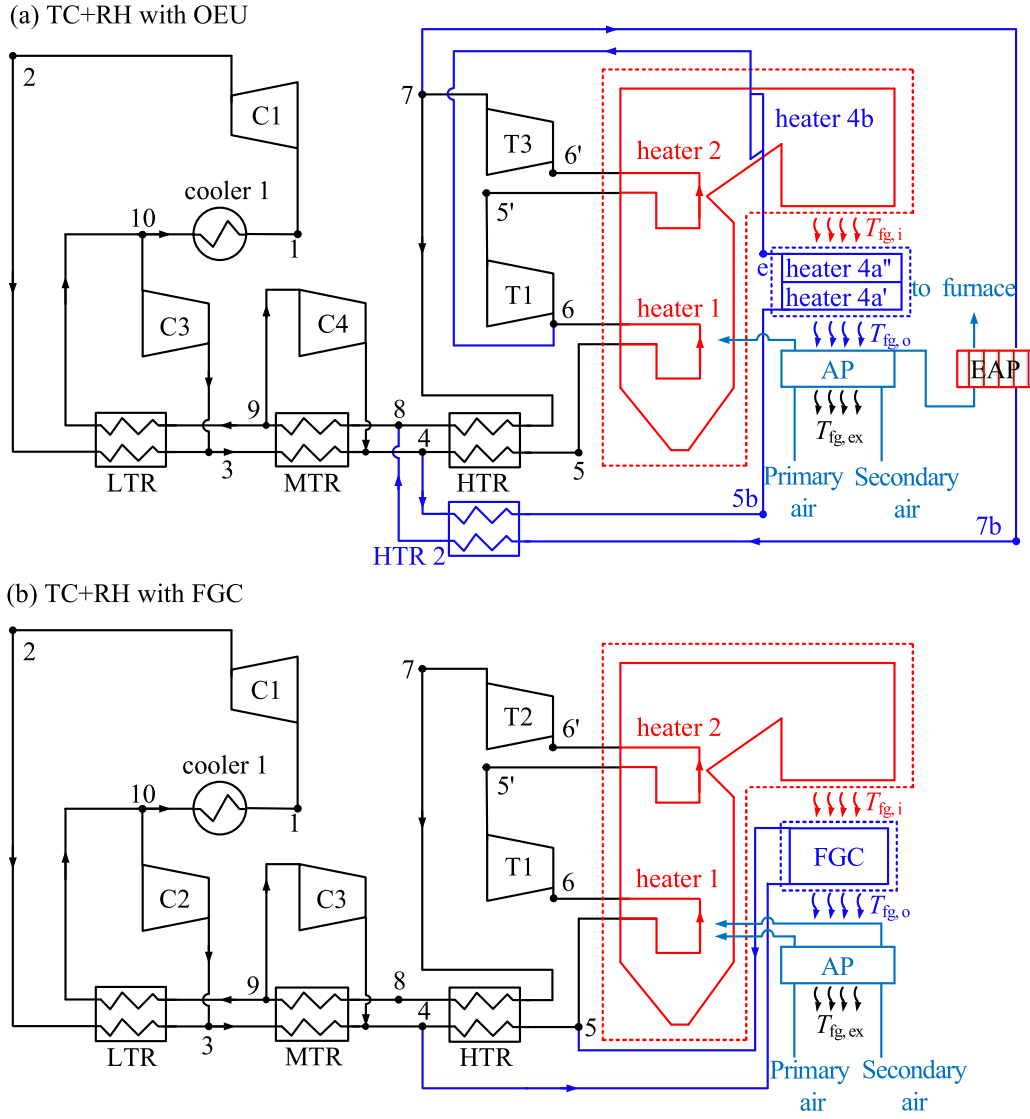


Fig. 8. Tri-compressions plus reheating (TC + RH) adapting to OEU (a) and FGC (b).

Table 3 [26]). Flue gas exergy e_{fg} is calculated as follows:

$$e_{fg} = h_{fg} - T_0 s_{fg} h_{fg} = \sum_{i=1}^M \phi_i h_i + h_{fh} s_{fg} = \sum_{i=1}^M \phi_i s_i + s_{fh} \quad (15)$$

where s_{fg} is the entropy of flue gas per unit mass of coal, h_{fh} and s_{fh} are enthalpy and entropy of fly ash after unit mass coal fired, M are the species of flue gas, including CO_2 , SO_2 , N_2 , O_2 , H_2O steam, ϕ_i is the ratio of the volume of i -th species to the total flue gas volume.

The exergy loss in boiler components equals to the input exergy of flue gas subtracting the output exergy of fluid (CO_2 or air). As an example for FGC, I_{FGC} is

$$I_{FGC} = B_{cal} (e_{fg,i} - e_{fg,o}) - x_{FGC} m_{CO_2} (e_4 - e_3) \quad (16)$$

where $e_{fg,i}$ and $e_{fg,o}$ are the flue gas exergy at FGC inlet and outlet, respectively.

3.2. Computation of sCO_2 boiler

Boiler shall be coupled with cycle computation, including the determination of heat losses and pressure drops. The boiler efficiency η_{boiler} is calculated by the anti-balance method [38]:

$$\eta_{boiler} = 1 - (Q_2 + Q_3 + Q_4 + Q_5 + Q_6) / Q_r \quad (17)$$

where Q_2 , Q_3 , Q_4 , Q_5 and Q_6 are the heat losses due to outlet flue gas discharged to environment, unburned gases, unburned carbon, heat dissipation to environment, ash per unit mass of coal, respectively, Q_r is the input energy per unit mass of coal.

Pressure drops in boiler tubes consists of components of friction (ΔP_f), gravity (ΔP_g) and acceleration (ΔP_a) [37]

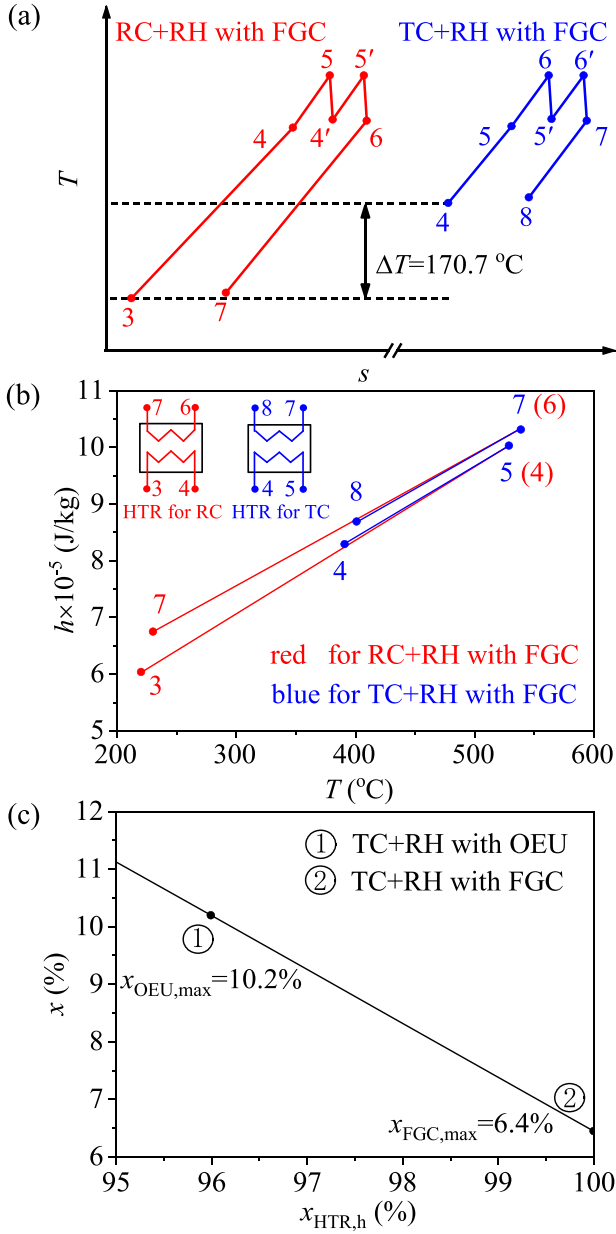


Fig. 9. Comparison of RC and TC on the extraction of moderate temperature flue gas energy (a: T - s curves showing elevated temperature level during heat absorption process; b: h - T curves in HTR (high temperature recuperator heat exchanger) for RC + RH and TC + RH; c: relationship of CO_2 flow rate ratio in heat exchangers operating in moderate temperature flue gas region and CO_2 flow rate ratio in high temperature side of HTR).

$$\begin{cases} \Delta P = \Delta P_f + \Delta P_g + \Delta P_a \\ \Delta P_a = G^2 \left(\frac{1}{\rho_o} - \frac{1}{\rho_i} \right) \\ \Delta P_g = \rho g H \end{cases} \quad (18)$$

where ρ_o and ρ_i are the CO_2 densities at the outlet and inlet of corresponding component, respectively, G is the mass flux, g is the acceleration of gravity, H is the height of the component. ΔP_f is [37]

$$\Delta P_f = \frac{1}{2} f \frac{l}{d_i} \frac{G^2}{\rho_b} \quad (19)$$

where l is the length of component, d_i is the inner diameter of tube, f is the friction coefficient [39]:

$$f = \frac{1}{3.24 l g^2 \left[\left(\frac{\Delta/d_i}{3.7} \right)^{1.11} + \frac{6.9}{Re_f} \right]} \quad (20)$$

where Δ is the roughness of tube wall ($\Delta = 0.012$ mm for stainless-steel tube), Re_f is the Reynolds number. CO_2 in boiler tubes significantly deviate from pseudo-critical point to behave gas-like characteristic. Thus, convective heat transfer coefficient in tubes is calculated by the D-B correlation [40]:

$$h_f = \frac{\lambda_f}{d_i} 0.023 Re_f^{0.8} Pr_f^{0.4} \quad (21)$$

where λ_f and Pr_f are the thermal conductivity and Prandtl number of CO_2 , respectively.

4. Results and discussion

4.1. The analysis for RC + RH with OEU and FGC

When using RC + RH, the major difference between OEU and FGC lies in different pressure drops and exergy destructions in various components. With a constraint of 123°C for outlet flue gas temperature ($T_{\text{fg,ex}}$), Fig. 4 shows $T \sim \Delta H$ curves, where ΔH is the enthalpy change along heat transfer route. Focusing on moderate and low temperature regions, OEU reaches a pinch temperature of 30°C for heater 4a in moderate temperature region, with a 40°C temperature difference between flue gas and CO_2 in the opposite site of heater 4a (see Fig. 4a). However, FGC attains larger temperature difference between flue gas and CO_2 in the range of $(134\text{--}164)^\circ\text{C}$ (see Fig. 4b). The temperature match between the two sides of fluids for AP is similar for both OEU and FGC applications.

Our previous study shows that the enclosed area of $T \sim \Delta H$ curves between two sides of fluids represents the magnitude of exergy destruction [41]. Regarding Fig. 4, heater 4a for OEU has the exergy destruction of 0.72 MW, but FGC accounts for an exergy destruction of 2.82 MW. The AP accounts for the exergy destruction of 2.94 MW for OEU and 3.05 MW for FGC. Then, we examine exergy destructions in the whole system in Fig. 5. The total exergy destructions are weakly changed between OEU and FGC applications, which are 114.44 MW for OEU and 115.00 MW for FGC. The combustion process has great contribution to exergy destruction, which accounts for 46.10% for OEU and 45.99% for FGC. The secondly large contribution comes from the heater components of boiler, which is 28.46% for OEU and 30.26% for FGC.

Attention is paid on pressure drops in various components of boiler. Pressure drops should be controlled to be as small as possible. This is because for given turbine inlet pressure, smaller pressure drops in various heat exchangers decrease the output pressure of compressor, which decreases the compression work for compressor. Among the three components of pressure drops, friction pressure drop dominates the

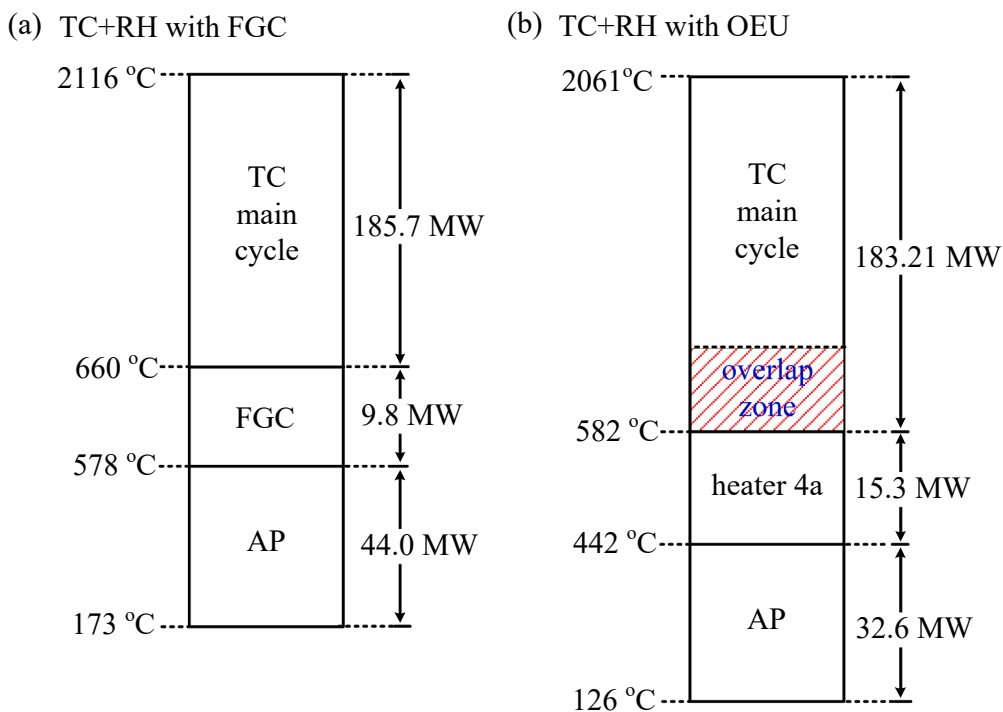


Fig. 10. Distributions of flue gas temperature and thermal loads (a: cascade energy utilization for TC + RH, b: overlap energy utilization for TC + RH).

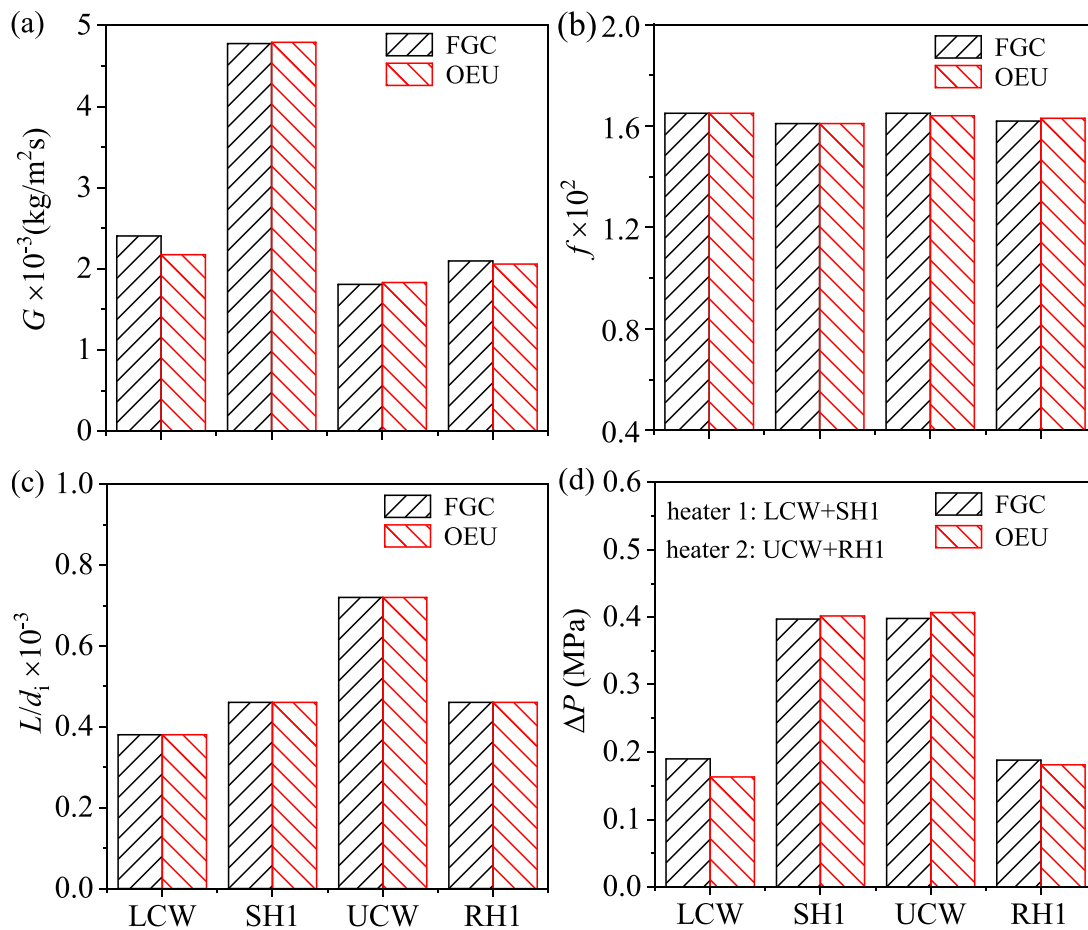


Fig. 11. Factors influencing pressure drops for TC + RH with OEU and FGC (a: mass fluxes in tubes; b: frictional coefficients; c: length to diameter ratio of tubes; d: frictional pressure drops in boiler components).

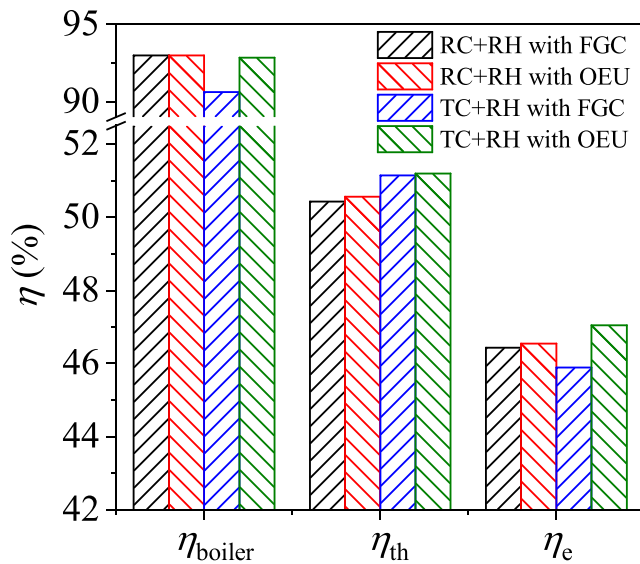


Fig. 12. Boiler efficiency, thermal efficiency and electric power efficiency for RC + RH and TC + RH with FGC and OEU.

contribution to the total pressure drop. Thus, friction pressure drop is examined. Fig. 6 plots mass flux G , friction coefficient f , length to diameter ratio L/d_i and friction pressure drop ΔP_f in components of LCW (lower part of cooling wall), SH1 (superheater 1), UCW (upper part of cooling wall), RH1 (reheater 1). Because OEU slightly decreases mass fluxes in LCW, SH1 and RH1 (see Fig. 6a), the final outcome yields the decreased pressure drops in these components (see Fig. 6d).

We note that the electric power efficiency of the whole system η_e is the outcome of thermal efficiency η_{th} timing the boiler efficiency η_{boiler} . Because both OEU and FGC can keep the same outlet flue gas temperature of 123 °C, boiler efficiency is the same. Compared with FGC, OEU slightly decreases pressure drops in boiler components, causing a slight thermal efficiency improvement. The final outcome yields an electric power efficiency improvement of 0.13% due to the utilization of OEU compared with FGC (see Fig. 7).

4.2. The analysis for TC + RH with OEU and FGC

TC uses three compressors and three recuperators instead of two for RC. Fig. 8a shows TC + RH with OEU after performing components sharing of top and bottom cycle. Both two cycles use TC + RH and OEU ensures same pressure and temperature for some components of two cycles. $T_{\text{fig},i}$, $T_{\text{fig},o}$ and $T_{\text{fig},ex}$ are called the interface temperatures among the three regions of flue gas energies. Heaters 1, 2 and 4b are responsible for the extraction of high temperature flue gas energy. Heater 4a and AP account for the extraction of moderate and low temperature flue gas energies. Similar to RC + RH with OEU (see Fig. 1), an overlap region is set in high temperature zone for TC + RH with OEU and flue gas energies in this subzone are not only absorbed by top cycle, but also by bottom cycle, which ensures no efficiency gap between top cycle and bottom cycle.

Alternatively, Fig. 8b shows TC + RH with FGC. A portion of CO₂ flow rate from C3 outlet in a sCO₂ cycle flows through the FGC, heated by moderate temperature flue gas, and then mixes with the main CO₂

stream at the inlet of heater1. Similar with RC + RH with FGC (see Fig. 2b), the three regions of flue gas energies are extracted by the main TC + RH cycle, a FGC and an AP respectively.

In Fig. 9a, the heat absorption processes are marked as 3–4–5–4'–5'–6 for RC, and 4–5–6–5'–6'–7 for TC, concluding higher thermal efficiency by using TC instead of RC, due to the elevated temperature level of the heat absorption process by TC. One notes that the electric power efficiency not only depends on thermal efficiency of a cycle, but also depends on the boiler efficiency. Because TC elevates the CO₂ temperature level in cycle side to decrease the temperature difference between flue gas and CO₂, a question may be asked that does TC have sufficient capability to extract flue gas energy over entire temperature range? To answer to this question, x is defined as the ratio of the CO₂ flow rate in heat exchanger operating in moderate temperature flue gas region (that heat exchanger is FGC for FGC application, or heater 4a for OEU application), to the total CO₂ flow rate. $x_{\text{HTR},h}$ is the ratio of CO₂ flow rate in high temperature side of HTR to the total CO₂ flow rate. For RC + RH with FGC, we have

$$x_{\text{FGC,RC}} = 1 - \frac{h_6 - h_7}{h_4 - h_3}, \quad q_{\text{FGC,RC}} = x_{\text{FGC,RC}}(h_4 - h_3) \quad (22)$$

Alternatively, for TC + RH with FGC, we have

$$x_{\text{FGC,TC}} = 1 - \frac{h_7 - h_8}{h_5 - h_4}, \quad q_{\text{FGC,TC}} = x_{\text{FGC,TC}}(h_5 - h_4) \quad (23)$$

where $q_{\text{FGC,RC}}$ and $q_{\text{FGC,TC}}$ are the thermal loads of FGC when using RC or TC respectively, referenced to unit mass flow rate of CO₂. The comparison of the second term of right side of Eqs. 22 and 23 judges which cycle (RC or TC) keeps larger heat load for FGC. Hence, the CO₂ enthalpies for both high temperature side and low temperature side are plotted in Fig. 9b. Compared with the enthalpy lines of 6–7 and 3–4 (red color) for RC, TC narrows the angle between the two lines of 7–8 and 5–4 (blue color). Hence, the second term of $(h_6 - h_7)/(h_4 - h_3)$ for RC is smaller than $(h_7 - h_8)/(h_5 - h_4)$ for TC, concluding the decreased heat absorption capability in moderate temperature flue gas region by using TC instead of RC, when FGC is integrated in the system.

Fig. 9c shows the linearly decreased CO₂ flow rate for the extraction of moderate temperature flue gas energy versus the CO₂ flow rate in high temperature side of HTR. Specifying the pinch temperature limit of 10 K for HTR yields the maximum CO₂ flow rate ratio, which is 10.2% for OEU and 6.44% for FGC. Compared with FGC, OEU increases the energy extraction capability in moderate temperature flue gas region. OEU not only has higher thermal efficiency of the system, but also overcomes the shortcoming of the deteriorated performance for the extraction of moderate temperature flue gas energy.

Fig. 10 presents the outcomes for TC + RH when adapting to FGC and OEU. The TC + RH cycle extracts the high and moderate temperature flue gas energies, in which FGC or heater 4a can be considered as the subsystem of the TC + RH cycle. Because TC elevates the CO₂ temperature level to decrease temperature difference between CO₂ of cycle side and flue gas of furnace side, the thermal load by FGC is not preferable. Meanwhile, AP cannot account for sufficient thermal load. Thus, the outlet flue gas temperature discharged to environment is 173 °C, which is not acceptable. Alternatively, OEU increases the CO₂ flow rate in heater 4a (see Fig. 9c), enhancing the thermal load in moderate temperature flue gas region. With the help of air-preheater (AP), the outlet flue gas temperature can be 126 °C, which is acceptable.

Friction pressure drops of boiler for TC is analyzed in Fig. 11.

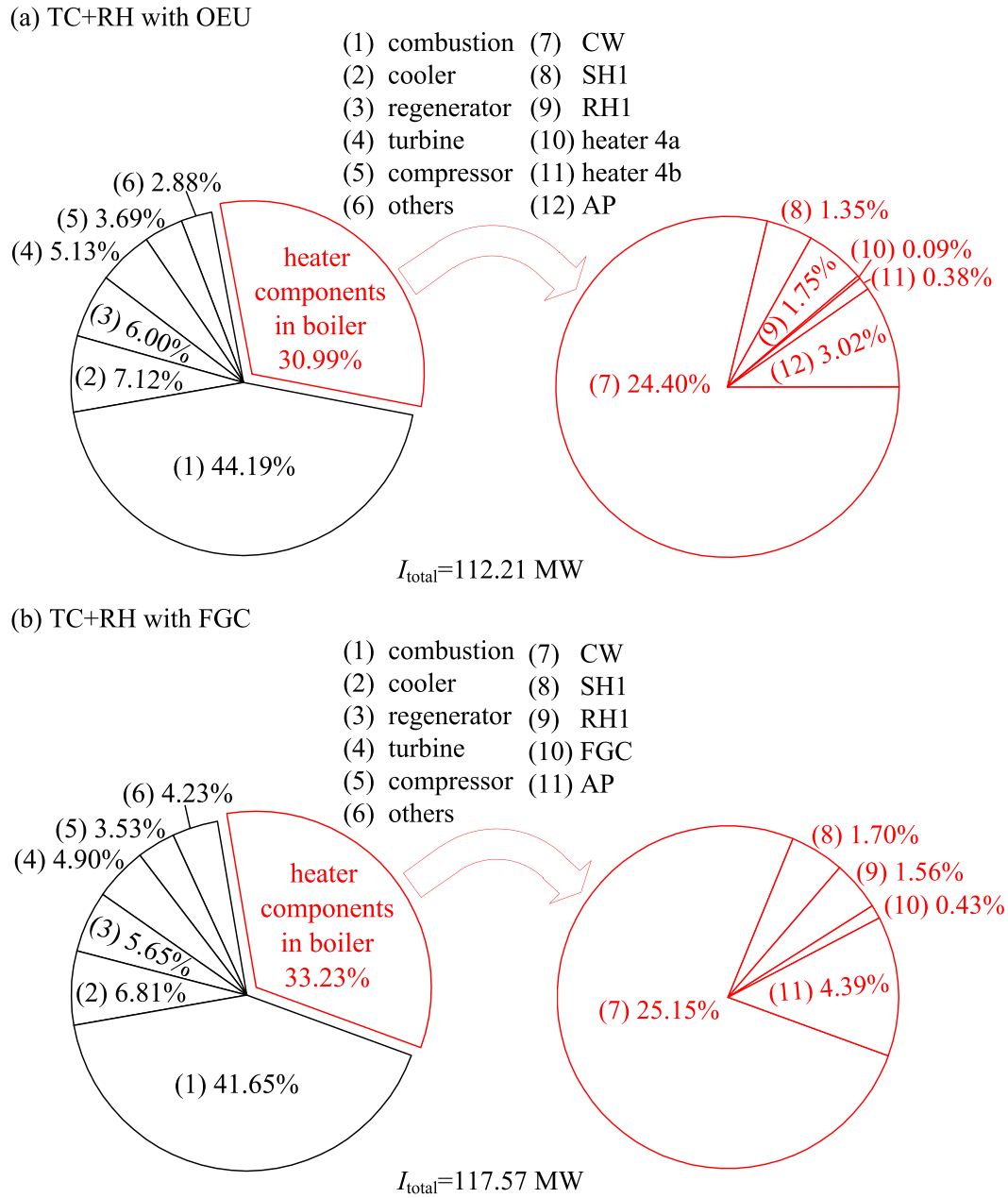


Fig. 13. Exergy destruction distributions for TC + RH with OEU (a) and FGC (b).

Comparing FGC and OEU, mass fluxes in various components are similar, except that G slightly decreases in LCW for OEU, resulting in slightly decreased pressure drops in LCW for OEU (see Fig. 6d). The efficiency of TC and RC systems are compared in Fig. 12. Color in black, red, blue and green columns represent RC + RH with FGC, RC + RH with OEU, TC + RH with FGC, TC + RH with OEU respectively. The mini difference of pressure drops between FGC and OEU for TC yields similar thermal efficiency η_{th} , which is 51.19% for OEU and 51.14% for FGC, which are obviously higher than RC system. However, the higher outlet flue gas temperature for TC + RH with FGC lowers the boiler efficiency to 90.64%, which is smaller than other three systems. This difference of

boiler efficiency causes the electric power efficiency of 47.05% for TC + RH with OEU and 45.89% for TC + RH with FGC.

Finally, we examine the exergy destructions for TC, which is 112.21 MW for OEU, and 117.57 MW for FGC (see Fig. 13). The mini difference of exergy destructions is caused by the fact that the combustion process dominates the exergy destructions in the system. However, the two methods to extract the moderate temperature flue gas energies change the exergy destructions contribution of boiler components, which is 30.99% when using OEU, due to the decreased temperature difference between CO_2 and flue gas, and 33.23% when using FGC.

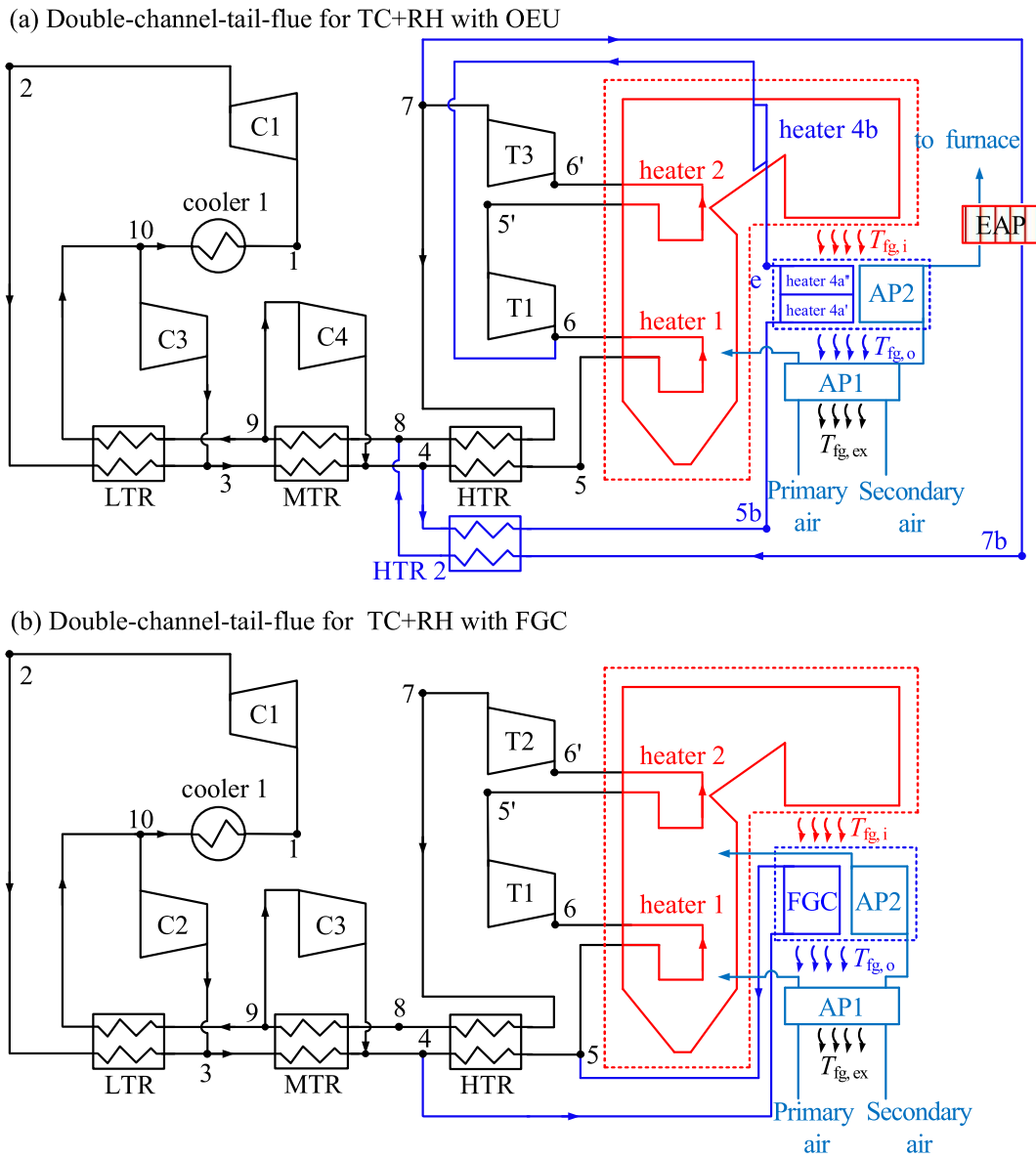


Fig. 14. The double-channel-tail-flue concept for TC + RH adapting to OEU (a) and FGC (b).

Table 1
Parameters for the cycle computations and boiler design.

Parameters	Values
Cycle type	Indirect
boiler type	Pulverized coal boiler
Net power (W_{net})	100 MWe
Inlet temperature of compressor C1	32 °C
Inlet pressure of compressor C1	7.6 MPa
Inlet temperature of turbine T1	620 °C
Inlet pressure of turbine T1	28 MPa
Turbines isentropic efficiency [37]	0.91
Compressors isentropic efficiency [37]	0.89
Pressure drop in regenerator [26]	0.1 MPa
Pinch temperature difference in regenerator [26]	10 °C
Primary air temperature entering air preheater	31 °C
Primary air temperature leaving air preheater	320 °C
Ratio of primary air flow rate to the total air flow rate	0.19
Secondary air temperature entering air preheater	23 °C
Ratio of secondary air flow rate to the total air flow rate	0.81
Environment temperature	20 °C
Excess air coefficient	1.2
Pinch temperature difference between flue gas and CO ₂	30 °C

4.3. The method to increase the flue gas energy extraction when using TC cycle

The above section demonstrates that TC increases the CO₂ temperature level during heat absorption due to the increased degree of recuperation heat within the system. Thus the system thermal efficiency is improved compared with RC. Even though TC introduces difficulty in absorbing moderate temperature flue gas energy, OEU still can decrease the outlet flue gas temperature to a reasonable level, but FGC cannot do that to worsen the boiler efficiency.

To overcome this issue, a double-channel-tail-flue technique is introduced (see Fig. 14). The purpose is to enjoy both the benefits of higher thermal efficiency of the system and higher boiler efficiency. Initially, the moderate flue gas energy is recovered by heater 4a for OEU or FGC only, the new design ensures such energy recovery is not only performed by heater 4a or FGC, but also by AP2 (air-preheater 2). AP1 still accounts for the low grade flue gas energy extraction. The total air flow rate after leaving AP1 is decoupled into two streams. The main stream directly returns to the furnace for combustion. The residual stream is continued to be heated by a portion of moderate flue gas energy and finally returns to furnace for combustion. In fact, the double-

Table 2
Equations and exergy destructions the RC + RH with OEU and FGC (the left column is cited from Ref. [37]).

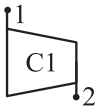
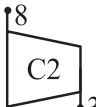
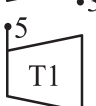
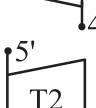

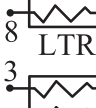


Components	RC + RH with OEU	RC + RH with FGC
	$\eta_{c,s} = \frac{h_{2s} - h_1}{h_2 - h_1}, w_{C1} = (1 - x_{C2})(h_2 - h_1); i_{C1} = w_{C1} - (1 - x_{C2})(e_2 - e_1)$	$\eta_{c,s} = \frac{h_{2s} - h_1}{h_2 - h_1}, w_{C1} = (1 - x_{C2})(h_2 - h_1); i_{C1} = w_{C1} - (1 - x_{C2})(e_2 - e_1)$
	$\eta_{c,s} = \frac{h_{3s} - h_8}{h_3 - h_8}, w_{C2} = x_{C2}(h_3 - h_8); i_{C2} = w_{C2} - x_{C2}(e_3 - e_8)$	$\eta_{c,s} = \frac{h_{3s} - h_8}{h_3 - h_8}, w_{C2} = x_{C2}(h_3 - h_8); i_{C2} = w_{C2} - x_{C2}(e_3 - e_8)$
	$\eta_{t,s} = \frac{h_5 - h_{4'}}{h_5 - h_{4's}}, w_{T1} = h_5 - h_{4'}; i_{T1} = e_5 - e_{4'} - w_{T1}$	$\eta_{t,s} = \frac{h_5 - h_{4'}}{h_5 - h_{4's}}, w_{T1} = h_5 - h_{4'}; i_{T1} = e_5 - e_{4'} - w_{T1}$
	$P_{5'} = \sqrt{P_5 P_6}, \eta_{t,s} = \frac{h_{5'} - h_6}{h_{5'} - h_{6s}}, w_{T2} = h_{5'} - h_6; i_{T2} = e_{5'} - e_6 - w_{T2}$	$P_{5'} = \sqrt{P_5 P_6}, \eta_{t,s} = \frac{h_{5'} - h_6}{h_{5'} - h_{6s}}, w_{T2} = h_{5'} - h_6; i_{T2} = e_{5'} - e_6 - w_{T2}$
	$T_8 = T_2 + \Delta T_{LTR}, x_{C2} = 1 - \frac{h_7 - h_8}{h_3 - h_2}, i_{LTR} = e_7 - e_8 - (1 - x_{C2})(e_3 - e_2)$	$T_8 = T_2 + \Delta T_{LTR}, x_{C2} = 1 - \frac{h_7 - h_8}{h_3 - h_2}, i_{LTR} = e_7 - e_8 - (1 - x_{C2})(e_3 - e_2)$
	$T_7 = T_3 + \Delta T_{HTR}, (1 - x_{EAP})(h_6 - h_7) = (1 - x_{Heater\ 4})(h_4 - h_3); i_{HTR} = (1 - x_{EAP})(e_6 - e_7) - (1 - x_{Heater\ 4})(e_4 - e_3)$	$T_7 = T_3 + \Delta T_{HTR}, (h_6 - h_7) = (1 - x_{FGC})(h_4 - h_3); i_{HTR} = (e_6 - e_7) - (1 - x_{FGC})(e_4 - e_3)$
	$x_{EAP}(h_{6b} - h_7) = x_{Heater\ 4}(h_{4b} - h_3); i_{HTR2} = x_{EAP}(e_{6b} - e_7) - x_{Heater\ 4}(e_{4b} - e_3)$	—
	$i_{Cooler} = (1 - x_{C2})(e_8 - e_1)$	$i_{Cooler} = (1 - x_{C2})(e_8 - e_1)$

Table 3
Properties of the designed coal [26].

C_{ar}	H_{ar}	O_{ar}	N_{ar}	S_{ar}	A_{ar}	M_{ar}	V_{daf}	Q_{LHV}
61.70	3.67	8.56	1.12	0.60	8.80	15.55	34.73	23,442

C (carbon), H (hydrogen), O (oxygen), N (nitrogen), S (sulfur), A (ash), M (moisture), V (volatile). Subscripts ar, d, af mean as received, dry and ash free, $C_{ar} + H_{ar} + O_{ar} + N_{ar} + S_{ar} + A_{ar} + M_{ar} = 100$.

channel-tail-flue technique is an overlap energy utilization in moderate temperature flue gas region. Fig. 15 presents a comparison between the systems with and without using the double-channel-tail-flue technique. For TC + RH with OEU, double-channel-tail-flue not only increases thermal load in moderate temperature flue gas region from 15.4 MW to 23.4 MW, but also decreases outlet flue gas temperature from 126 °C to 120 °C. The thermal load in low temperature flue gas region is similar, concluding more convenient utilization of moderate/low temperature flue gas energies by using double-channel-tail-flue technique. Double-channel-tail-flue significantly improves the performance for TC + RH with FGC, evidenced by the fact that it not only increases thermal load in moderate temperature flue gas region from 9.8 MW to 26.4 MW, but also

decreases outlet flue gas temperature from 173 °C to 120 °C. With the help of double-channel-tail-flue concept, FGC can satisfy the requirement for lower outlet flue gas temperature, corresponding to higher boiler efficiency, when adapting to TC + RH, but it cannot do that without double-channel-tail-flue technique.

5. Conclusions

Small capacity coal fired power plant using sCO₂ cycle is expected to have fast response to load variations, inspiring us to perform the present study. Driven by the improvement of system efficiency, this paper presents a comparison of RC, which is widely applied in the literature, and TC, which is proposed by the present authors recently. It is shown that, indeed, due to the elevated temperature level of the heat absorption process, TC is preferable than RC.

The second issue is the recovery of moderate/low temperature flue gas energies. The two methods of OEU and FGC are paid great attention. OEU refers to setting an overlap flue gas region, in which the flue gas energy is not only absorbed by the top cycle, but also by the bottom cycle. The components sharing simplified the system design. We show that when using RC + RH, both OEU and FGC have the capability to extract moderate temperature flue gas energy. OEU has a 0.13%

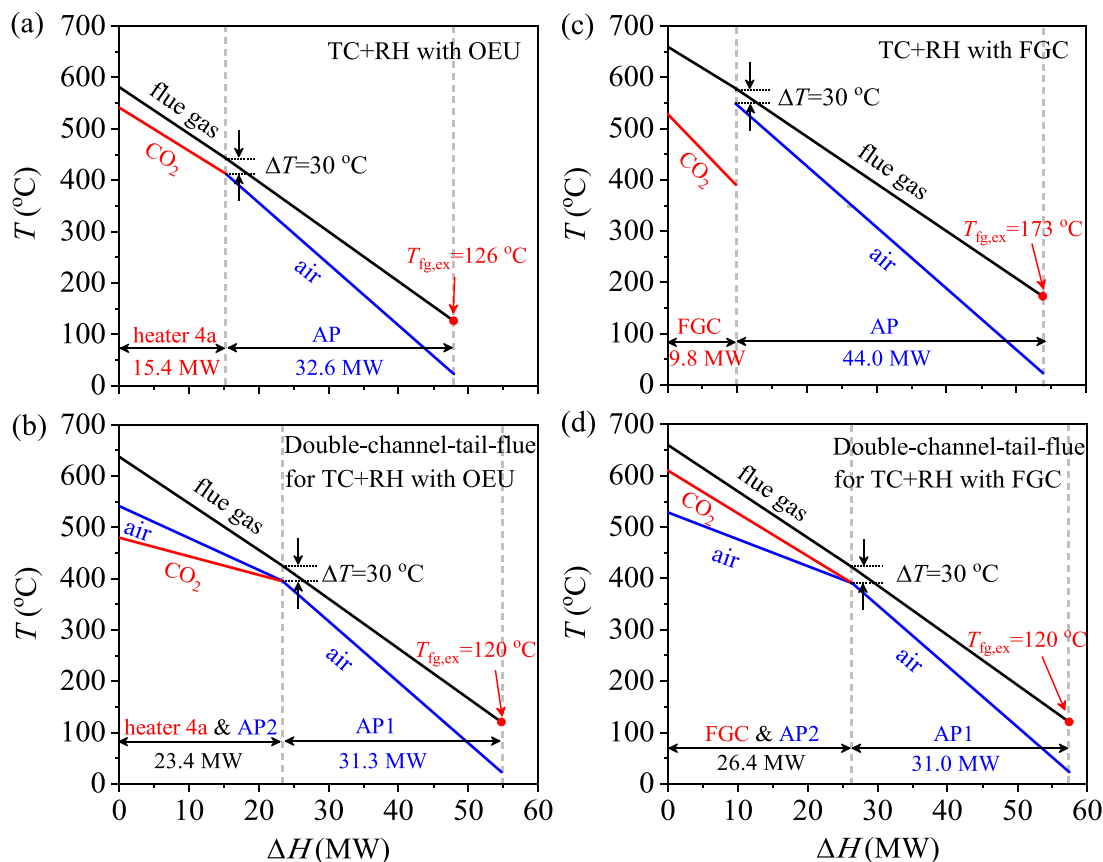


Fig. 15. T - ΔH curves for heat exchangers (heater 4a or FGC) operating in moderate temperature flue gas region and AP operating in low temperature flue gas region for TC + RH (a and c) and TC + RC with double-channel-tail-flue (b and d).

efficiency improvement compared with FGC, due to slightly decreased pressure drops in boiler components. Generally, both OEU and FGC can be adapted to RC + RH, and the system performance has weak difference between them.

The situation is changed when using TC instead of RC. Even though TC + RH introduces difficulty in absorbing moderate temperature flue gas energy, OEU, together with AP, can decrease the outlet flue gas temperature to 126 °C, which is acceptable practically. FGC has not sufficient capability to extract moderate temperature flue gas energy. The outlet flue gas temperature is 173 °C, inspiring us to propose the double-channel-tail-flue concept. An air-preheater (AP) is decoupled into two parts of AP1 and AP2. The former extracts low temperature flue gas energy. After leaving AP1, the air stream is segmented into two streams: one stream directly returns to furnace, but the other stream is warmed by a portion of moderate temperature flue gas energy. Hence, the system increases the capability to extract moderate/low temperature flue gas energy to decrease outlet flue gas temperature and raise boiler efficiency.

CRediT authorship contribution statement

Zhaofu Wang: Methodology, Software, Investigation, Writing – original draft. **Enhui Sun:** Conceptualization, Methodology, Writing – review & editing. **Jinliang Xu:** Conceptualization, Supervision, Funding acquisition, Writing – review & editing. **Chao Liu:** Methodology, Validation. **Guanglin Liu:** Formal analysis, Funding acquisition.

Declaration of Competing Interest

The authors declare that they have no known competing financial interests or personal relationships that could have appeared to influence the work reported in this paper.

Acknowledgements

This work was supported by Natural Science Foundation of China (52130608, 51821004), and the Key Laboratories for National Defense Science and Technology (No.6142702200510).

Appendix

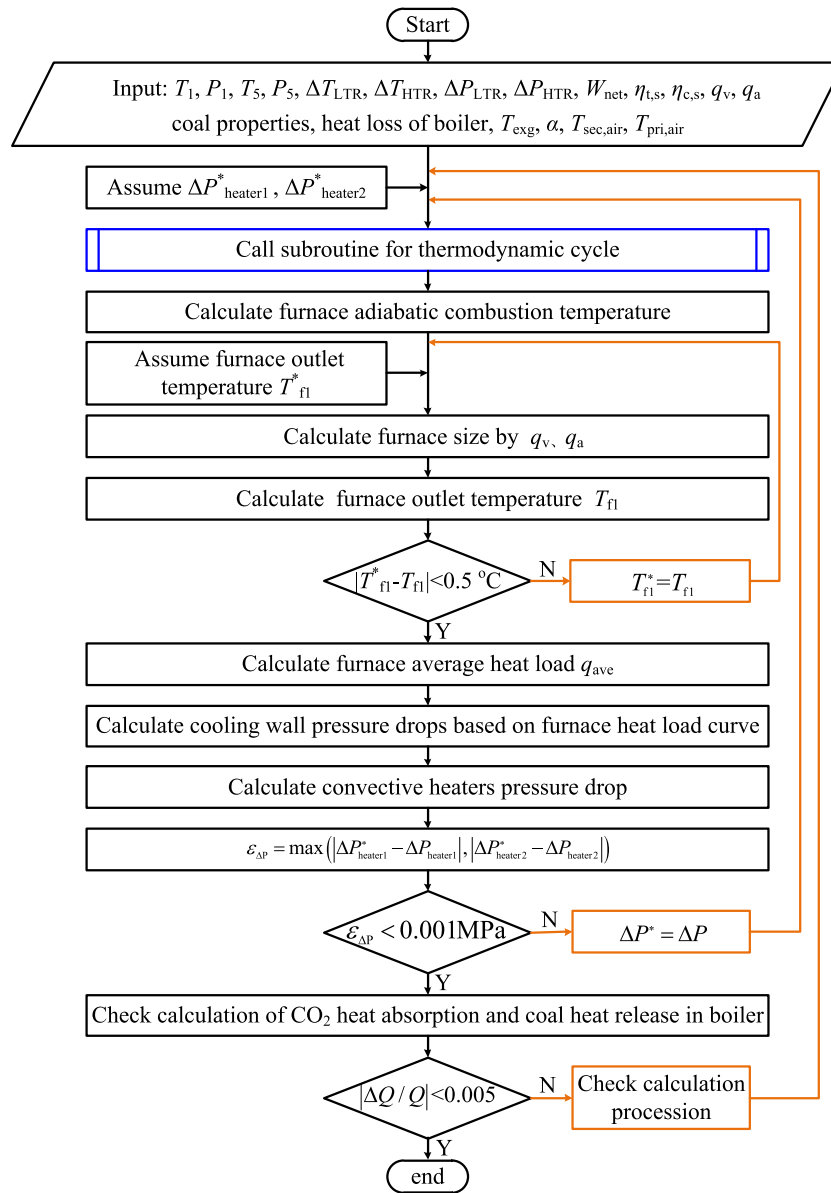


Fig. A1. Numerical calculations for recompression cycle coupling with boiler.

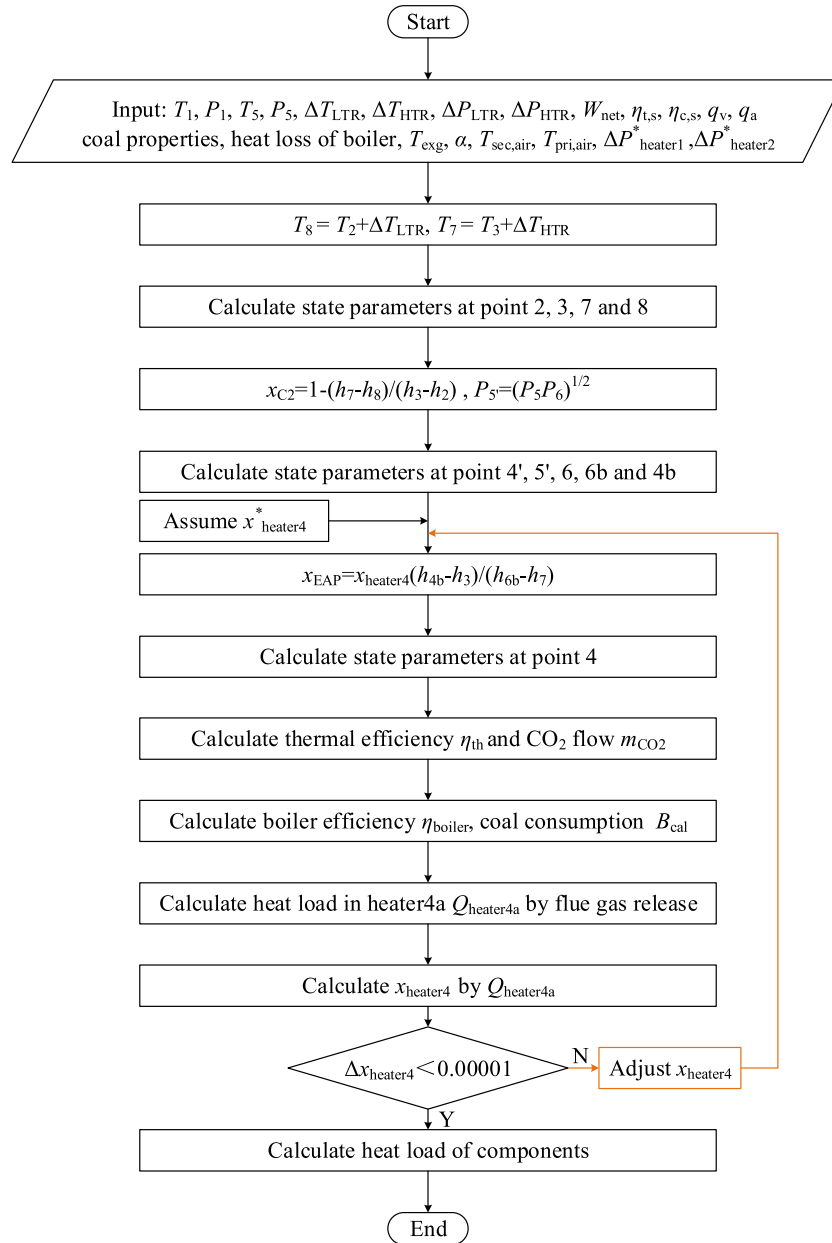


Fig. A2. Computation scheme of thermodynamic cycle based on overlap energy utilization (OEU).

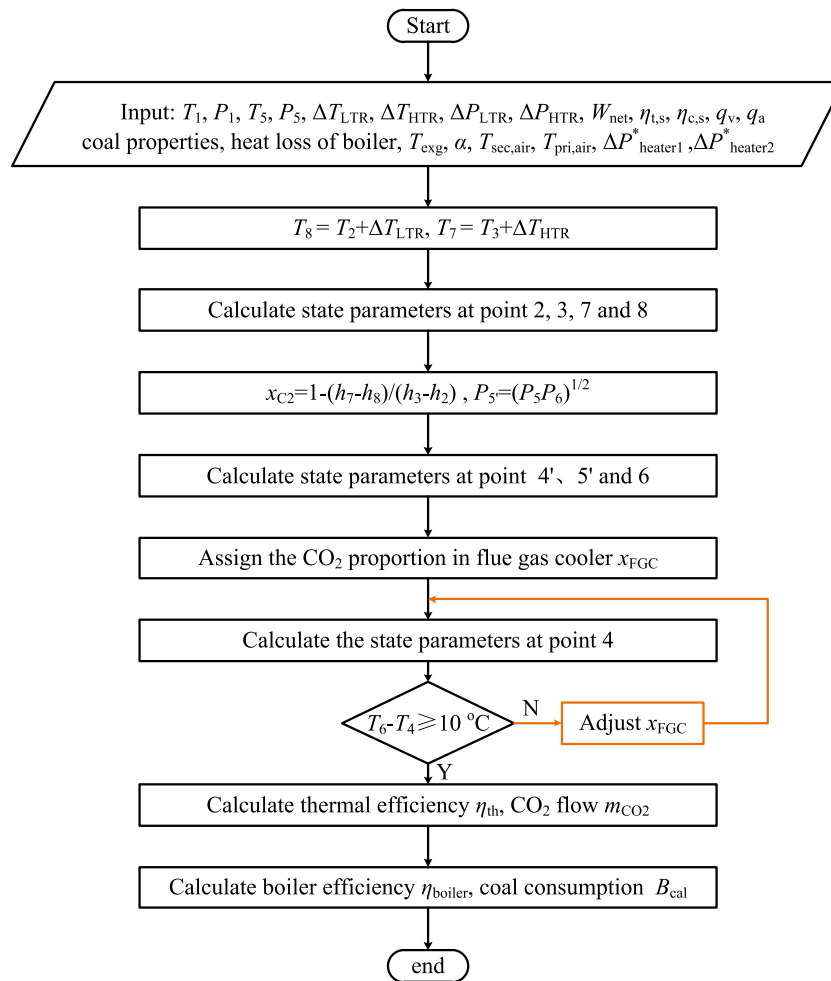


Fig. A3. Computation scheme of thermodynamic cycle based on adding a flue gas cooler (FGC).

References

- [1] White MT, Bianchi G, Chai L, Tassou SA, Sayma AI. Review of supercritical CO₂ technologies and systems for power generation. *Appl Therm Eng* 2021;185: 116447.
- [2] Yu A, Su W, Lin X, Zhou N. Recent trends of supercritical CO₂ Brayton cycle: Bibliometric analysis and research review. *Nucl Eng Technol*. 2021;53(3):699–714.
- [3] Dostal V. A supercritical carbon dioxide cycle for next generation nuclear reactors. Ph.D. thesis. USA: Department of Nuclear Engineering, Massachusetts Institute of Technology; 2004.
- [4] Luo C, Zhao F, Zhang Na. A novel nuclear combined power and cooling system integrating high temperature gas-cooled reactor with ammonia-water cycle. *Energy Convers Manage* 2014;87:895–904.
- [5] Park JH, Yoon J, Eoh J, Kim H, Kim MH. Optimization and sensitivity analysis of the nitrogen Brayton cycle as a power conversion system for a sodium-cooled fast reactor. *Nucl Eng Des* 2018;340:325–34.
- [6] Park JH, Park HS, Kwon JG, Kim TH, Kim MH. Optimization and thermodynamic analysis of supercritical CO₂ Brayton recompression cycle for various small modular reactors. *Energy* 2018;160:520–35.
- [7] Gao C, Wu P, Shan J, Huang Y, Zhang J, Wang L. Preliminary study of system design and safety analysis methodology for supercritical carbon dioxide Brayton cycle direct-cooled reactor system. *Ann Nucl Energy* 2020;147:107734. <https://doi.org/10.1016/j.anucene.2020.107734>.
- [8] Wang K, He Y-L. Thermodynamic analysis and optimization of a molten salt solar power tower integrated with a recompression supercritical CO₂ Brayton cycle based on integrated modeling. *Energy Convers Manage* 2017;135:336–50.
- [9] Javanshir A, Sarunac N, Razzaghpahan Z. Thermodynamic analysis of simple and regenerative Brayton cycles for the concentrated solar power applications. *Energy Convers Manage* 2018;163:428–43.
- [10] Singh R, Miller SA, Rowlands AS, Jacobs PA. Dynamic characteristics of a direct-heated supercritical carbon-dioxide Brayton cycle in a solar thermal power plant. *Energy*. 2013;50:194–204.
- [11] Yang J, Yang Z, Duan Y. Off-design performance of a supercritical CO₂ Brayton cycle integrated with a solar power tower system. *Energy*. 2020;201:117676. <https://doi.org/10.1016/j.energy.2020.117676>.
- [12] Linares JI, Montes MJ, Cantizano A, Sánchez C. A novel supercritical CO₂ recompression Brayton power cycle for power tower concentrating solar plants. *Appl Energy* 2020;263:114644. <https://doi.org/10.1016/j.apenergy.2020.114644>.
- [13] Ruiz-Casanova E, Rubio-Maya C, Pacheco-Ibarra JJ, Ambriz-Díaz VM, Romero CE, Wang X. Thermodynamic analysis and optimization of supercritical carbon dioxide Brayton cycles for use with low-grade geothermal heat sources. *Energy Convers Manage* 2020;216:112978. <https://doi.org/10.1016/j.enconman.2020.112978>.
- [14] Li Bo, Wang S-S, Wang K, Song L. Comparative investigation on the supercritical carbon dioxide power cycle for waste heat recovery of gas turbine. *Energy Convers Manage*. 2021;228:113670. <https://doi.org/10.1016/j.enconman.2021.113670>.
- [15] Tozlu A, Abuşoğlu A, Özahi E. Thermo-economic analysis and optimization of a Recompression supercritical CO₂ cycle using waste heat of Gaziantep Municipal Solid Waste Power Plant. *Energy* 2018;143:168–80.
- [16] Pan P, Yuan C, Sun Y, Yan X, Lu M, Bucknall R. Thermo-economic analysis and multi-objective optimization of S-CO₂ Brayton cycle waste heat recovery system for an ocean-going 9000 TEU container ship. *Energy Convers Manage* 2020;221: 113077. <https://doi.org/10.1016/j.enconman.2020.113077>.
- [17] Yang D, Tang G, Fan Y, Li X, Wang S. Arrangement and Three-Dimensional Analysis of Cooling Wall in 1000 MW S-CO₂ Coal-fired Boiler. *Energy*. 2020;197: 117168.
- [18] Olumayegun O, Wang M, Oko E. Thermodynamic performance evaluation of supercritical CO₂ closed Brayton cycles for coal-fired power generation with solvent-based CO₂ capture. *Energy*. 2019;166:1074–88.
- [19] Liese E, Albright J, Zitney SA. Startup, shutdown, and load-following simulations of a 10 MWe supercritical CO₂ recompression closed Brayton cycle. *Appl Energy*. 2020;277:115628. <https://doi.org/10.1016/j.apenergy.2020.115628>.
- [20] Li H, Zhang Y, Yao M, Yang Y, Han W, Bai W. Design assessment of a 5 MW fossil-fired supercritical CO₂ power cycle pilot loop. *Energy* 2019;174:792–804.
- [21] Le Moulec Y. Conceptual study of a high efficiency coal-fired power plant with CO₂ capture using a supercritical CO₂ Brayton cycle. *Energy* 2013;49:32–46.
- [22] O'Shaughnessy E, Heeter J, Shah K, Koebrich S. Corporate acceleration of the renewable energy transition and implications for electric grids. *Renew Sust Energy Rev* 2021;146:111160. <https://doi.org/10.1016/j.rser.2021.111160>.
- [23] Bird L, Lew D, Milligan M, Carlini EM, Estanqueiro A, Flynn D, et al. Wind and solar energy curtailment: A review of international experience. *Renew Sust Energy Rev* 2016;65:577–86.

- [24] Xu J, Liu C, Sun E, Xie J, Li M, Yang Y, et al. Perspective of S-CO₂ power cycles. *Energy* 2019;186:115831. <https://doi.org/10.1016/j.energy.2019.07.161>.
- [25] Kim YM, Sohn JL, Yoon ES. Supercritical CO₂ Rankine cycles for waste heat recovery from gas turbine. *Energy* 2017;118:893–905.
- [26] Xu J, Sun E, Li M, Liu H, Zhu B. Key issues and solution strategies for supercritical carbon dioxide coal fired power plant. *Energy* 2018;157:227–46.
- [27] Mecheri M, Le Moullec Y. Supercritical CO₂ Brayton cycles for coal-fired power plants. *Energy* 2016;103:758–71.
- [28] Zhang Y, Li H, Han W, Bai W, Yang Yu, Yao M, et al. Improved design of supercritical CO₂ Brayton cycle for coal-fired power plant. *Energy* 2018;155:1–14.
- [29] Bai W, Zhang Y, Yang Y, Li H, Yao M. 300 MW boiler design study for coal-fired supercritical CO₂ Brayton cycle. *Appl Therm Eng* 2018;135:66–73.
- [30] Park S, Kim J, Yoon M, Rhim D, Yeom C. Thermodynamic and economic investigation of coal-fired power plant combined with various supercritical CO₂ Brayton power cycle. *Appl Therm Eng* 2018;130:611–23.
- [31] Sun E, Xu J, Li M, Liu G, Zhu B. Connected-top-bottom-cycle to cascade utilize flue gas heat for supercritical carbon dioxide coal fired power plant. *Energy Convers Manage*. 2018;172:138–54.
- [32] Sun E, Xu J, Hu H, Li M, Miao Z, Yang Y, et al. Overlap energy utilization reaches maximum efficiency for S-CO₂ coal fired power plant: A new principle. *Energy Convers Manage*. 2019;195:99–113.
- [33] Li H, Zhang Y, Yang Y, Han W, Yao M, Bai W, et al. Preliminary design assessment of supercritical CO₂ cycle for commercial scale coal-fired power plants. *Appl Therm Eng* 2019;158:113785. <https://doi.org/10.1016/j.applthermaleng.2019.113785>.
- [34] Halimi B, Suh KY. Computational analysis of supercritical CO₂ Brayton cycle power conversion system for fusion reactor. *Energy Convers Manage*. 2012;63:38–43.
- [35] Sun E, Xu J, Li M, Li H, Xie J. Synergetics: The cooperative phenomenon in multi-compressions S-CO₂ power cycles. *Energy Convers Manage X*. 2020;7:100042.
- [36] Marion J, Kutin M, McClung A, Mortzheim J, Ames R. The STEP 10 MWe sCO₂ Pilot Plant Demonstration. In: ASME, editor. Proceedings of ASME Turbo Expo 2012: Turbine Technical Conference and Exposition, Phoenix, Arizona, USA, Denmark; June 17–21, 2019.
- [37] Liu C, Xu J, Li M, Wang Z, Xu Z, Xie J. Scale law of sCO₂ coal fired power plants regarding system performance dependent on power capacities. *Energy Convers Manage*. 2020;226:113505. <https://doi.org/10.1016/j.enconman.2020.113505>.
- [38] Fan Q. Boiler principle. Beijing: China Electric Power Press; 2014 [in Chinese].
- [39] Wang Z, Sun B, Wang J, Hou L. Experimental study on the friction coefficient of supercritical carbon dioxide in pipes. *Int J Greenhouse Gas Conf* 2014;25:151–61.
- [40] Yang S, Tao W. Heat transfer. Beijing: Higher Education Press; 2006 [in Chinese].
- [41] Yu C, Xu J, Sun Y. Transcritical pressure Organic Rankine Cycle (ORC) analysis based on the integrated-average temperature difference in evaporators. *Appl Therm Eng* 2015;88:2–13.